VOL. 11, NO. 6, MARCH 2016 ISSN 1819-6608
ARPN Journal of Engineering and Applied Sciences

www.arpnjournals.com

EFFECT OF FORCE PROFILES OF DIFFERENT ELECTRODE ACTUATION SYSTEMS TO WELD STRENGTH

Aravinthan Arumugam
School of Engineering, KDU University College, Utropolis, Glenmarie, Jalan Kontraktor, Seksyen, Selangor, Malaysia
E-Mail: aravinthan.a@kdu.edu.my

ABSTRACT

Studies were carried out on the force profiles of the pneumatic electrode actuation system and servo electrode actuation system to analyse their effects on weld strength. The studies were carried out at three different locations of the weld lobe; below the lower limit, between the lower limit and upper limit and above the upper limit. Servo electrode actuation system was able to produce weld with better strength compared to the pneumatic electrode actuation system within the weld lobe, due to its ability to produce high resistance for the same welding current. Below the lower limit, servo electrode actuation system was able to produce a sound weld with the use of a low welding current combined with a preferred failure mode. Similarly above the upper limit, servo electrode actuation system was able to produce a weld with high current and without the occurrence of expulsion. Finally, it was observed that with the servo electrode actuation system, the width of the pneumatic electrode actuation system's weld lobe can be improved to an extent.

Keywords: electrode actuation system, weld lobe, dynamic resistance, welds strength.

INTRODUCTION

Spot welding process parameters

Resistance spot welding (RSW) is a process used to join sheet metals by means of a series of spot welds. The quality of a spot weld can be determined based on the achieved weld strength. The three main parameters that influence spot weld strength are current, time and force. Proper control of these parameters will produce the required heat for melting the metals and facilitate the development of the spot weld. Increase in spot weld diameter has been shown to increase spot weld strength (Aravinthan and Nachimani, 2011). Increase in the welding current increases the weld diameter, which in turn increases the weld strength until expulsion occurs (Aslanlar *et al*., 2007). Similarly increase in weld time also increases weld diameter and weld strength until occurrence of expulsion (Pouranvari and Marashi, 2010). On the other hand, decrease in electrode force will increase the weld diameter and the weld strength until expulsion occurs (Zhang *et al.*, 2009).

Effect of electrode force on dynamic resistance, expulsion and weldability lobe

Electrode force plays a huge role in the heat generation during the spot welding process according to the equation (Sun *et al*., 2007), (Zhou and Chai, 2014):

$$Q = I^2 \times R \times t \quad (1)$$

where Q = heat generated (kJ), I = welding current (kA), R = resistance (Ω) and t = weld time (cycles - 1 cycles = 20 ms for a 50 Hz spot welding machine). During the weld cycle, electrode force influences the dynamic resistance, which produces the Joule heating required for spot weld growth. The dynamic resistance during welding was reported to correlate well to the weld nugget growth as shown in Figure-1 (Dickinson *et al.,* 1980). The β-peak indicates the start of weld nugget growth. The dynamic resistance was found to decrease with an increase in electrode force during welding (Wen *et al*., 2009). The delay in the formation of the β-peak at higher electrode force also indicates a delay in the initiation of weld nugget growth due to the reduction in Joule heating.

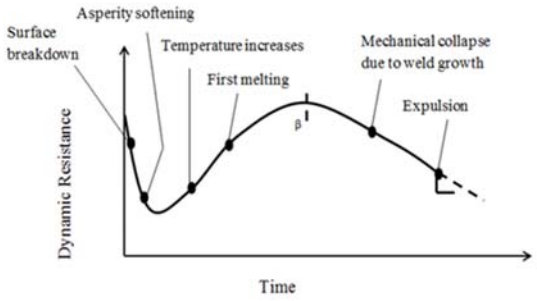

Figure-1. Dynamic resistance curve (Dickinson *et al.* 1980).

Expulsion occurs as molten metal erupts from the weld area due to reasons such as extreme high current, longer weld time, lower electrode force, improper surface condition and presence of gap between metal sheets and misalignment between electrodes and metal sheets. Severe expulsion has been reported to cause reduction in weld strength and cause damages to metal surface and welding electrode (Shen *et al*., 2010), (Gjazanfari and Naderi, 2014). Electrode force was also found to affect the

weldability lobe curves. Weldability lobe curves give the combination of welding current and time that will give an acceptable weld at constant force. Different combinations of welding current and weld time below the lower curve and above the upper curve will give undersized welds and welds with expulsion, respectively. These welds are unacceptable when weld strength is a concern. Sun (Sun *et al*., 2007) mentioned that the width of the weldability lobe is affected by the change in electrode force. Recently, dynamic controls of the electrode force during welding with the use of servomechanism have been reported by various authors (Liang, Liu and Bai, 2011), (Iyota *et al*., 2014), (Ikeda *et al*., 2012). However, no work have been reported to have compared the ability of the conventional pneumatic electrode actuation system and servo electrode actuation system in producing sound welds at various locations of the weldability lobe. Therefore, the aim of this work will be to compare the effect of the force profiles from both these systems to the spot weld diameter and strength, at different locations of a weld lobe. The work will also discuss on the possibility of improving the weld lobe of a pneumatic system with the use of a servo system.

EXPERIMENTATION

Instrumentation

A pedestal type welding machine with a pneumatic electrode actuation system was retrofitted into a servo electrode actuation system in this work. In the servo electrode actuation system, unlike in the pneumatic actuation system where a piston head was used to move the electrode, a ball screw was used to convert the rotary motion of the servomotor to a linear motion so that the electrode can be actuated upward and downward. Piezoelectric force-strain sensor was fitted to the lower arm of the machine to measure the applied electrode force based on the strain produced at the lower arm. Precaution was taken to ensure that the location where the sensor is fitted will give a close representation of the applied electrode force. This is due to the infeasibility of measuring the electrode force directly from the electrode tip during the welding process. The electrodes used in this work are RWMA Class II CuCr alloy electrodes with tips of 6 mm in diameter. Test samples for metallographic study and tensile tests were prepared from mild steel sheets with dimensions of 100 mm x 30 mm and thickness of 2 mm. For the tensile test samples, two sheets were placed on top of each other with an overlap of 30 mm.

Development of weld lobe for different electrode forces

Initially, weld lobes for the welding machine with the pneumatic system were developed using three different electrode forces; 1.5 kN, 2.5 kN and 3.5 kN. Figure-2 shows the developed weld lobes. When the electrode force increases, the weld lobe moves upward indicating that when electrode force increases, either the current or the weld time needs to be increased for acceptable weld growth.

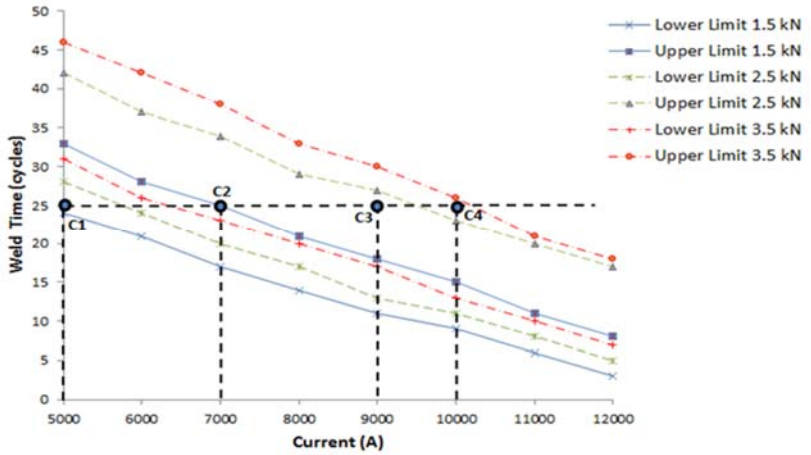

Figure-2. Weld lobes for three different electrode forces.

Data acquisition and force control systems

Data acquisition system was used to capture the signals from the piezoelectric sensor to plot the electrode force profiles during welding. Dynamic control of electrode force during welding was not possible in the pneumatically driven welding system (Niu, Chi and Zhang, 2009). However, implementing a force control system was possible in the servo actuated spot welding machine. A proportional-integral-derivative (PID) controller was developed to control the electrode force during the weld cycle based on predefined force profiles as shown in Figure-3. The force control performances on various force profiles have been tested and evaluated. Details on the force controller and the satisfactory performances of the system were reported in (Aravinthan and Baharuddin, 2014).

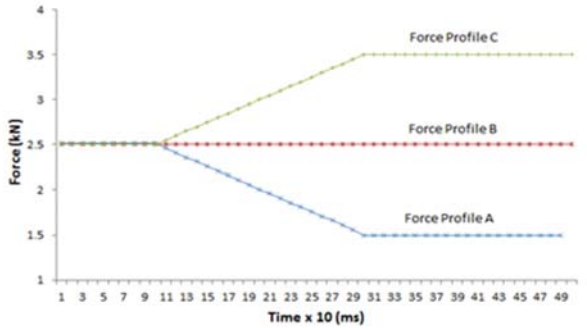

Figure-3. Force profiles for servo electrode actutation system.

Three different force profiles were used in this work. Force profile A is a varying force profile which starts at electrode force of 2.5 kN at the start of the weld cycle, changes to 1.5 kN in the middle of the weld cycle and remains at that force till the end of the weld cycle. Force profile B is a constant force profile which remains at 2.5 kN throughout the weld cycle. Finally, force profile C is a varying force profile which starts at electrode force of 2.5 kN at the start of the weld cycle, changes to 3.5 kN in the middle of the weld cycle and remains at that force till the end of the weld cycle. This force profiles where chosen with the 2.5 kN weld lobe in Figure-2 as a reference.

Comparison in weld growth for different electrode actuation systems at various locations in the weld lobe

Three different experiments were carried out in this work at three different locations in the 2.5 kN weld lobe i.e. C1 (below the lower limit), C2 and C3 (within the upper and lower limits) and C4 (above the upper limit). The force profiles of both the pneumatic and servo electrode actuation systems and their effects on weld strengths on all these locations were examined in detail.

a) Within the upper and lower limits of the weld lobe

As the force within the weld lobe represent constant force, constant force experimentation was carried out to compare the weld growth in the pneumatic electrode actuation system and servo electrode actuation system. As in the case of the pneumatic system, the pressure gauge was set to 2 bar and force on the electrode tips was repeatedly checked with the use of a hand held force gauge while the machine is in test mode. The gauge showed that the electrode force that was exerted on the sbeet metals is 2.5 kN. For the servo system, force profile B (constant force of 2.5 kN) as shown in Figure-3 was used. The weld time of 25 cycles (500 ms) and welding currents of 7 kA (C2) and 9 kA (C3) were used. Both these welding currents are within the 2.5 kN weld lobe. Seven repetitions were made on each electrode actuation systems.

b) Below the lower limit of the weld lobe

In this experimentation, the weld growth in a servo electrode actuation system which uses a varying force profile was compared with the weld growth in a pneumatic electrode actuation system, when welding was carried out below the lower limit of the weld lobe. The force profile A as shown in Figure-3 was used for the servo electrode actuation system. The reason for the use of this force profile was as seen in Figure-2. In order to produce a weld at C1, the electrode force needs to be changed from 2.5 kN to 1.5 kN. For the pneumatic spot welding machine, the electrode force was set at 2.5 kN. The weld time of 25 cycles (500 ms) and welding current of 5 kA (C1) were used. Seven repetitions were made on each electrode actuation systems.

c) Above the upper limit of the weld lobe

In this experimentation, the weld growth in a servo electrode actuation system which uses a varying force profile was compared with the weld growth in a pneumatic electrode actuation system, when welding was carried out above the upper limit of the weld lobe. The force profile C as shown in Figure-3 was used for the servo spot welding machine. The reason for the use of this force profile was in order to produce a weld at C4 without expulsion, the electrode force needs to change from 2.5 kN to 3.5 kN. For the pneumatic spot welding machine, the electrode force was set at 2.5 kN. The weld time of 25 cycles (500 ms) and welding current of 10 kA were used. Seven repetitions were made on each electrode actuation systems.

RESULTS AND DISCUSSIONS

The weld strengths were recorded from the tensile tests that were carried out using a Shimadzu tensile testing machine with a crosshead speed of 5 mm/min. The dynamic resistance curves in this work were generated based on the procedures described by Sun (Sun *et al*., 2008). The averages for the dynamic resistances and strengths were based on four repetitions. Metallographic samples were produced using the standard metallographic procedure. Optical microscopy was used to examine the fusion zones (FZ) in these samples which have coarse macrostructures due to melting and solidification (Aravinthan and Nachimani, 2011). The weld diameter is represented by the width of the FZ. As an example, Figure-4 shows the width of the FZ equivalent to weld diameter of 4.8 mm, with the use of force profile B at 9 kA. Three samples were used for the metallographic examinations to calculate the average weld nugget diameters for each experimentation.

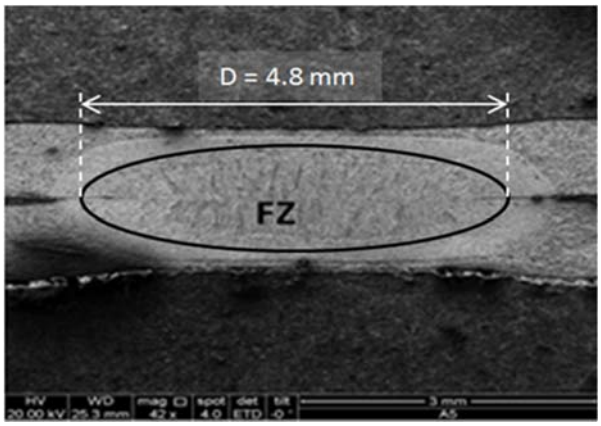

Figure-4. Weld diameter for force profile B at 9 kA.

Within the upper and lower limits of the weld lobe

a) Force profiles

Force profiles produced during the weld cycle for the electrode actuation systems are as shown in Figure-5.

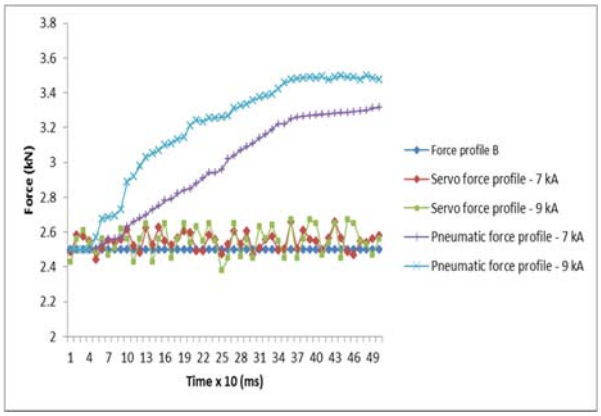

Figure-5. Force profiles for both electrode actuation systems within the weld lobe.

The electrode force for the pneumatic electrode actuation system, which was constant throughout the weld time without a weld being done, had a noticeable increase during welding. Similar observation was also reported by Ji and Zhou (Ji and Zhou, 2004) in their work. The increase in electrode force was found to be greater for the 9 kA welding current compared to the increase in electrode force for the 7 kA welding current. The increase in force during welding is because of the weld expansion during weld growth. Electrode force constrains the thermal expansion of the weld. However, when thermal expansion increases due to increase in welding current, a larger reaction force will overcome the electrode force; which will be shown as an increase in force. As reaction force increases with increase in current, the force increase for 9 kA was higher than the force increase in 7 kA. This also concludes that the electrode force profiles in a pneumatic system are process dependent. As in the case of the servo electrode actuation system, as shown in Figure-5, electrode force during welding was closely following the force profile B. A tolerance band of ± 0.2 kN was given to each force profile used in this work to take into account the noise that will be generated during the weld cycle. A low pass filter has been added to suppress the effect of the unwanted noise during welding.

b) Dynamic resistance and weld strength

Dynamic resistances for the electrode actuation systems are as shown in Figure-6. Firstly, a distinct separation between the dynamic resistance curves from the servo electrode actuation system (s) and dynamic resistance curves from the pneumatic electrode actuation system (p) was observed. The dynamic resistance curves from the servo electrode actuation system are higher than those from the pneumatic electrode actuation system. This is because the electrode force during welding in the servo system is lower than the electrode force in the pneumatic system as seen in Figure-5. This observation was similar to that reported by Wen (Wen *et al.*, 2009), which showed that electrode force is inversely proportional to dynamic resistance. Secondly, the dynamic resistance curves from the pneumatic electrode actuation system showed a drastic drop in resistance at the start of the weld cycle as compared to the dynamic resistance curves belonging to the servo electrode actuation system. This drastic drop is associated with the breakdown of contact insulations due to localized melting (Yanhua *et al.*, 2013). The drastic drop, however, was not noticed in the dynamic resistance curves for the servo system. The possible explanation to this is that during localized heating, electrode in the pneumatic based system has the tendency to further penetrate downwards when the material has melted due to the air pressure on the piston. This therefore may lead to a drastic reduction in resistance due to a faster increase in electrode force.

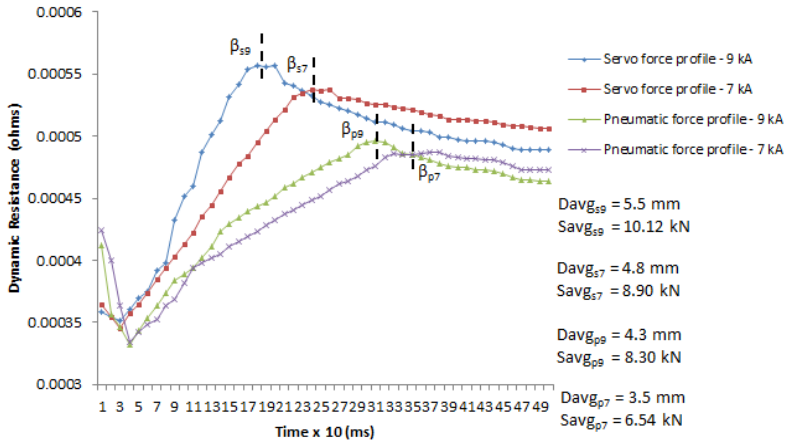

Figure-6. Dynamic resistance curves, weld strengths and weld diameters for both electrode actuation systems at 7 kA and 9 kA.

In a servo based system, since the electrode is connected to a ball screw, the lower movement of the electrode due to localized melting is restricted. As also seen in Figure-6, for both 9 kA and 7 kA welding currents, β-peaks of the dynamic resistance curves for the servo electrode actuation system (s9 and s7) occurred earlier compared to the β-peaks of the dynamic resistance curves for the pneumatic electrode actuation system (p9 and p7). This indicated that weld nugget growth was initiated earlier in the servo electrode actuation system compared to the pneumatic electrode actuation system. This was confirmed from the tensile test and weld diameter results which are also shown in Figure-6. Based on (1) since servo system's force profiles showed higher increase in resistances, they would potentially generate more heat for melting to occur compared to pneumatic system's force profiles for the same welding current and weld time. The high heat generated by these force profiles, therefore facilitated faster weld initiations during welding and the welds had sufficient time to grow, which in turn produced weld nuggets with bigger weld diameters (5.5 mm and 4.8 mm for 9 kA and 7 kA, respectively) and higher strengths (10.12 kN and 8.90 kN for 9kA and 7 kA, respectively).

Below the lower limit

a) Force profiles

Force profiles produced during the weld cycle for the electrode actuation systems are as shown in Figure-7. An increase in electrode force in the pneumatic electrode actuation system was observed during welding. The explanation for this is the same as discussed in the 'within the upper and lower limits' section. However, since the welding current used is 5 kA, the average increase in electrode force was found to be only about 0.5 kN compared to average increases of about 0.8 kN and 1 kN for welding currents of 7 kA and 9 kA, respectively. For the servo actuation system, as noticed in the 'within the upper and lower limits' section, the PID controller was able to control the electrode force during weld cycle to follow the force profile A and within the set tolerance band.

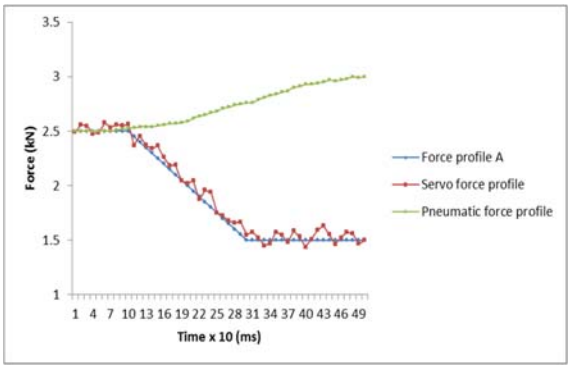

Figure-7. Force profiles for both electrode actuation systems below the lower limit of the weld lobe.

b) Dynamic resistance and weld strength

Dynamic resistances for the electrode actuation systems are as shown in Figure-8. The dynamic resistance curve for the servo electrode actuation system showed an increase in dynamic resistance mainly due the decreasing force profile which reduces the electrode force from 2.5 kN to 1.5 kN during the weld cycle. As the force profile starts reducing in force after 100 ms, a steep increase in resistance was noticed in the dynamic resistance curve. The observed β–peak indicated that the force profile facilitated weld nugget growth in the mid of the weld cycle even though a low welding current was used. As in the case of the pneumatic electrode actuation system, there was no obvious β–peak observed in the dynamic resistance curve. Hence, it was deduced that the increase in electrode force during welding together with the use of a low current delayed weld nugget growth, which led to the

development of a smaller and weaker weld than its counterpart, as can be seen in Figure-8. Comparing the failure mode of both welds, it also showed that the servo force profile produced a button pullout failure while the pneumatic force profile made the weld to fail by interfacial failure. Pouranvari *et al* (Pouranvari *et al*., 2011) mentioned in their work that the button pullout failure is the desirable failure mode due to its high energy absorption capability. The conclusion of this experimentation showed that with the use of servo electrode actuation system, it is possible to produce sound welds below the weld lobe's lower limit.

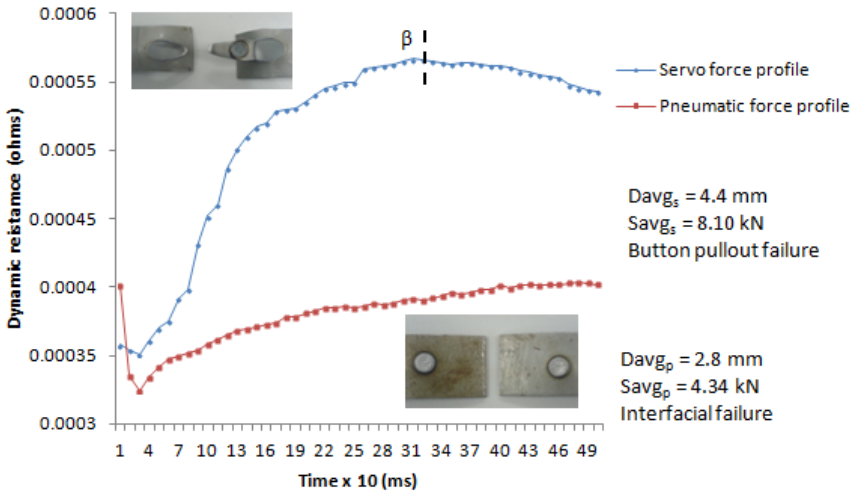

Figure-8. Dynamic resistance curves weld strengths and weld diameters for both electrode actuation systems at 5 kA.

Above the upper limit

a) Force profiles

Force profiles produced during the weld cycle for the electrode actuation systems are as shown in Figure-9.

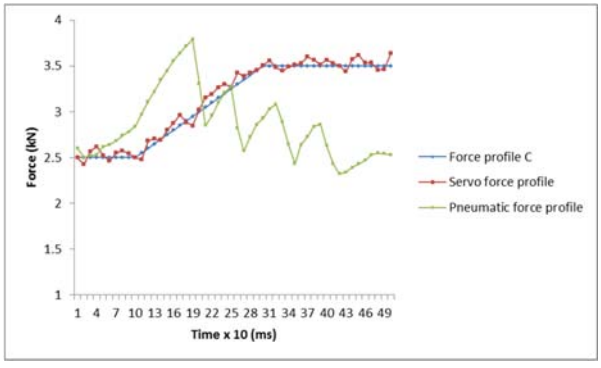

Figure-9. Force profiles for both electrode actuation systems above the upper limit of the weld lobe.

An interesting observation from Figure-9 is that of the force change during welding for the pneumatic electrode actuation system. Due to the use of an extreme current of 10 kA, expulsion occurred during welding. Force increase at the start of the welding process was similar to those seen in the previous two experiments. However, a drastic drop in the electrode force followed by a jagged pattern force change thereafter relates to the expulsion that was observed during welding. For the servo actuation system, the PID controller was able to control the electrode force during the weld cycle, to follow the force profile C and within the set of tolerance band. As the increase in electrode force in the servo electrode actuation system coincides with the drastic drop of electrode force in the pneumatic electrode actuation system, the force increase inhibited the occurrence of expulsion. Ability to suppress expulsion by increasing electrode force have also been discussed by Zhou and Chai (Zhou and Chai, 2014) and Shen *et al* (Shen *et al*., 2011) in their work.

b) Dynamic resistance and weld strength

Dynamic resistances for the electrode actuation systems are as shown in Figure-10. The dynamic resistance curves for both electrode actuation systems showed rapid increase in resistance at the early stage of weld cycle due to the use of a high current. In the dynamic resistance curve for the pneumatic electrode actuation system, after the β-peak was observed, there was a drastic drop in resistance, the time which coincides with the drastic drop in force due to expulsion. It is therefore concluded that the drastic drop in resistance is mainly due to expulsion, where overheating will cause the electrode to penetrate into the metal excessively leading to a high electrode indentation. In the case of the servo electrode actuation system, β-peak was observed at a resistance

higher than the β-peak for the pneumatic system but the β-peaks for both systems occurred at times which are closer to each other. This shows that for the 10 kA current, weld starts to develop at an average time of 140 ms. however the resistance drop in the servo electrode actuation system is mainly due to the increase in electrode force from 2.5 kN to 3.5 kN, unlike in the case of the pneumatic electrode actuation system. The increasing force profile used in this experimentation prevented the occurance of expulsion. Therefore the servo electrode actuation system produced weld with higher weld strength compared to the pneumatic electrode actuation system, even though the average weld diameters for both systems are quite close to each other as shown in Figure-10. Zhang (Zhang *et al.*, 2007) reported that when the indentation exceeds 20% of the part thicknesses, severe expulsion will occur leading to reduction in weld strength. This might have been the reason for the reduction in weld strength which was obtained using the pneumatic system.

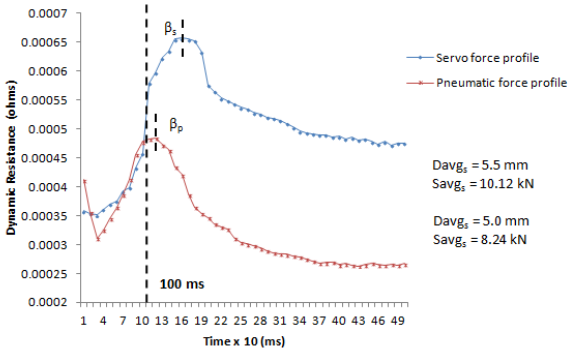

Figure-10. Dynamic resistance curves, weld strengths and weld diameters for both electrode actuation systems at 10 kA.

Weld lobe modification using varying force profiles

From the experimentations above, it was certain that the varying force profiles can be used to improve the lower limit and the upper limit of a weld lobe which was produced with the pneumatic system. The decreasing force profile was able to produce sound weld with the desired failure mode below the lower limit, while the increasing force profile was able to suppress expulsion at high current above the upper limit. The lower and upper limits of the 2.5 kN weld lobe was recreated using force profile A for the lower limit and force profile C for the upper limit. From Figure-11, it is observed that both force profiles expands the width the of 2.5 kN weld lobe but with some limitations. Force profile A, cannot be used at high currents i.e. currents above 9 kA. This is because as this force profile reduces force from 2.5 kN to 1.5 kN during welding, at high currents this causes expulsion to occur due to overheating and very low electrode force. Severe expulsion were noticed from 10 kA onwards even at very short weld time, therefore 10 kA onwards were considered 'unweldable' currents with the force profile used. On the other side, force profile C cannot be used at lower currents i.e. current below 9 kA. The reason for this is as this force increases from 2.5 kN to 3.5 kN during welding, at lower currents and higher electrode force, longer weld time are required for welds to be produced. As in terms of productivity, this is not acceptable.

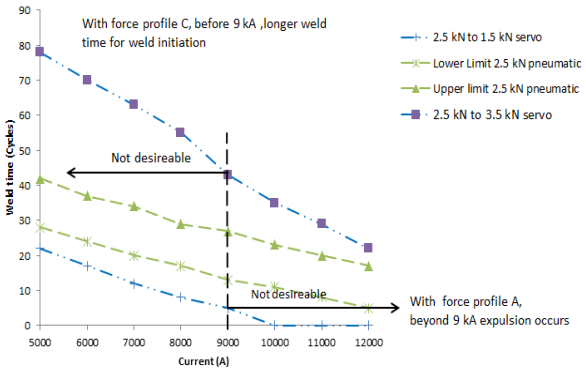

Figure-11. With force profile A and C before and beyond 9kA respectively.

CONCLUSIONS

Effect of the force profiles from the pneumatic electrode actuation system and servo electrode actuation system on weld strengths at different locations of the weld lobe have been analysed. The conclusions of the work are as below:

a) Within the upper limit and lower limit of the weld lobe, servo electrode actuation system produced a bigger weld diameter and stronger weld strength compared to the pneumatic electrode actuation system.

b) Below the lower limit of the weld lobe, the servo electrode actuation system which uses a force profile that reduces in force during welding produces a weld with nugget pullout failure mode.

c) Above the upper limit of the weld lobe, the servo electrode actuation system which uses a force profile that increases in force during welding was able to prevent occurance of expulsion.

d) The servo electrode actuation system was able to expand the weld lobe of a pneumatic electrode actuation system to an extent. However the use of the reducing force profile causes expulsion at higher currents and the increasing force profile extended the weld time at lower currents.

REFERENCES

Aravinthan, A. and Nachimani, C. 2011. Analysis of spot weld growth on mild and stainless steel. Welding Journal, 49, pp.143-147.

Aravinthan, A. and Baharuddin, A.A. 2014. Effect of force control during spot welding on weld properties. International Journal of Research and Scientific Publications. 4(8), pp.1-6.

Aslanlar, S., Ogur, A., Ozsarac, U. and Ilhan, E. 2007. Effect of welding current on mechanical properties of galvanized chromided steel sheet in electrical resistance spot welding. Materials and Design. 28, pp. 2-7.

Dickinson, D.W., Franklin, J.E. and Stanya, A. 1980. Characterization of spot welding behavior by dynamic electrical parameter monitoring. Welding Research Supplement, pp.170-176.

Ghazanfari, H. and Naderi, M. 2014. Expulsion characterization in resistance spot welding by means of hardness mapping techniques. International Journal of Minerals, Metallurgy and Materials, 21(9), pp.1-4.

Ikeda, R., Okita, Y., Ono, M., Yasuda, K. and Terasaki, T. 2012. Effect of electrode force condition on nugget diameter and residual stress in resistance spot welded high-strength steel sheets. International Symposium on Materials Science and Innovation for Sustainable Society: Eco-Materials and Eco-Innovation for Global Sustainability (Eco-Mates 2011), 379, pp. 1-9.

Iyota, M., Mikami, Y., Hashimoto, T., Taniguchi, K., Ikeda, R. and Mochizuki, M. 2014. Development of advanced resistance spot welding process using control of electrode force and welding current during welding. Welding International, 28(1), pp.13-20.

Ji, C.T. and Zhou, Y. 2004. Dynamic Electrode Force and Displacement in Resistance Spot Welding of Aluminum. Journal of Manufacturing Science and Engineering. 126, pp. 605-610.

Liang, C., Liu, X. and Bai, Y. 2011. Effect of electrode force change on spot weld quality of AHSS using servo gun. Manufacturing Process Technology, 189-193, pp. 3359-3363.

Niu,B., Chi, Y.L and Zhang, H. 2009. Dynamic electrode force control of resistance spot welding robot. 2009 IEEE International Conference on Robotics and Biomimetics (Robio 2009), 1-4, pp. 2421-2426.

Pouranvari, M. and Marashi, S.P.H. 2010. Factors affecting mechanical properties of resistance spot welding. Materials Science and Technology, 261(1), pp.1137-1144.

Pouranvari, M., Mousavizadeh, S.M., Marashi, S.P.H., Goodarzi, M. and Ghorbani, M. 2011. Influence of fusion zone size and failure mode on mechanical performance of dissimilar resistance spot welds of AISI 1008 low carbon steel and DP600 advanced high strength steel. Materials and Design, 32, pp.1390-1398.

Shen, J., Zhang, Y.S. and Lai, X.M. 2010. Influence of initial gap on weld expulsion in resistance spot welding of dual phase steel. Science and Technology of Welding and Joining. 15(5), pp. 386-392.

Shen, J., Zhang, Y. and Lai, X. 2011. Effect of electrode force on expulsion in resistance spot welding with initial gap. Material Science Forum, pp.795-798.

Sun, H., Zhang, Y., Lai, X. and Chen ,G. 2008. On-line inspection of weld quality based on dynamic resistance curve in resistance spot welding and weldbonding. Fourth International Symposium on Precision Mechanical Measurements. doi: 10.1117/12.819597.

Sun, H.T., Lai, X.M., Zhang, Y.S. and Shen, J. 2007. Effect of variable electrode force on weld quality in resistance spot welding. Science and Technology of Welding and Joining. 12(8), pp.718-724.

Wen,J., Wang, C.S., Xu, G.C. and Zhang, X.Q. 2009. Real time monitoring weld quality of resistance spot welding for stainless steel. ISIJ International, 49(4), pp. 553-556.

Yanhua, M., Pei, W., Chuanzhong, X., Yongan,Z. and He, S. 2013. Review on Techniques for On-Line Monitoring of Resistance Spot Welding Process. Advances in Materials Science and Engineering. pp. 1-6.

Zhang, X., Chen, G., Zhang Y. and Lai, X. 2009. Improvement of resistance spot weldability for dual-phase (DP600) steel using servo gun. Journal of Materials Processing Technology, 209, pp.2671-2675.

Zhang, Y.S., Zhang, X.Y., Lai, X.M. and Chen, G.L. 2007. Online quality inspection of resistance spot welded joint based on electrode indentation using servo gun. Science and Technology of Welding and Joining, 12(5), pp.449-454.

Zhou, K. and Cai, L. 2014. Study on effect of electrode force on resistance spot welding process. Journal of applied physics. 116.